PREPARATION OF PIGMENTS FOR SPACE-STABLE THERMAL CONTROL COATINGS

September 1970 through January 31, 1971

Contract No. NAS8-21317
Funded Under Code 124-09-18-1200-25-9-004-028-2510

Interim Report

Prepared by

W. B. Campbell
S. G. Nychas
R. G. Smith

of

The Ohio State University
Research Foundation
Columbus, Ohio

to

NATIONAL AERONAUTICS AND SPACE ADMINISTRATION

George C. Marshall Space Flight Center
Marshall Space Flight Center, Alabama

February 1971

PREPARATION OF PIGMENTS FOR SPACE-STABLE THERMAL CONTROL COATINGS

September 1970 through January 31, 1971

Contract No. NAS8-21317
Funded Under Code 124-09-18-1200-25-9-004-028-2510

Interim Report

Prepared by

W. B. Campbell
S. G. Nychas
R. G. Smith

of

The Ohio State University
Research Foundation
Columbus, Ohio

to

NATIONAL AERONAUTICS AND SPACE ADMINISTRATION

George C. Marshall Space Flight Center
Marshall Space Flight Center, Alabama

February 1971

ABSTRACT

Calculations of mixing conditions in the vapor reaction system established criteria for reactor design. Gas mixing was optimized by jet action and vapor phase production of zinc orthotitanate has been accomplished.

descriptors:

Thermal control space-stable pigments, Vapor phase, Nucleation, Zinc Orthotitanate, Ceramics, Gas mixing calculations.

FOREWORD

This report was prepared by The Ohio State University Research Foundation, under NASA Contract No. NAS8-21317, entitled, "Preparation of Pigments for Space-Stable Thermal Control Coatings." This report covers the period from September 30, 1970 through January 31, 1971
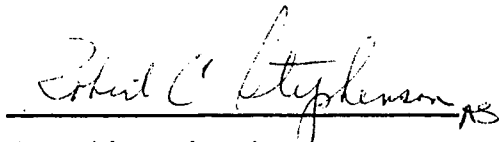
Major contributors to the program during this period were Dr. William B. Campbell, Principal Investigator; S. G. Nychas for mixing studies and reactor design, R. G. Smith and J. E. Seaver for vapor phase apparatus development and powder production.

<div align="right">

Respectfully submitted,
OSU Research Foundation

William B. Campbell, Ph.D.
Associate Professor

</div>

Approved:

Executive Director
OSU Research Foundation

SUMMARY

    Two major limitations previously found to retard the production
of multiple oxides and rare earth compounds; gas mixing and halide
generation have been studied. Calculations of mixing conditions estab-
lished the criteria for reactor design. This design has been incor-
porated into an existing furnace and zinc orthotitanate produced.

TABLE OF CONTENTS

LIST OF FIGURES

LIST OF TABLES

PREPARATION OF PIGMENTS FOR SPACE-STABLE THERMAL CONTROL COATINGS

I. INTRODUCTION

The development of vapor phase technology in the preparation of
space-stable pigments has been demonstrated by the production of rutile
powders having discrete morphology [1,2]. Systematic variations of
particle size were controlled with hot zone temperature, residence time,
and injector design [2]. The current investigation was designed to
study the production of stable pigments for thermal control coatings.
Materials include zinc titanates, calcium tungstate and lanthanum oxide.

Two major limitations retarding the production of multiple oxides
and rare earth compounds; gas mixing and halide generation have been
studied. A detailed mixing study has been performed and a reactor
designed from the results of this study. Halide generation problems
have been alleviated by the utilization of metallo-organic compounds
and/or localized induction heating.

II. EXPERIMENTAL PROCEDURE

A. Reactor Design, Mixing and Heat Transfer

Prior experience in the area of particle production by vapor phase reaction has shown that mixing of reactants was limited. To improve the mixing of reactant gases, a detailed study was performed and the results were used to design a reactor to provide suitable mixing of the gaseous species.

1. Thermodynamic and Transport Properties

The design of a reactor for the production of calcium tungstate, $CaWO_4$, in a gas phase system was based on the overall reaction.

$$CaCl_2 + WCl_5 + 7/2\ H_2 + 4CO_2 = 4CO + CaWO_4 + 7HCl \qquad (1)$$
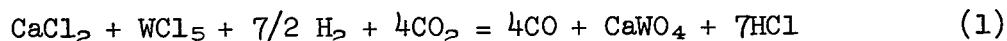
Energy balances, fluid mechanical, mixing and heat transfer calculations require the knowledge of thermodynamic and transport properties. Densities of reactants and products as well as heat capacities, viscosities, thermal conductivities and mass diffusivities were calculated or estimated whenever not available in literature. Classical thermodynamic calculations for the subject systems have been presented in earlier reports.

a. Viscosity

For the estimation of gas viscosity at low densities, the following formula was used [3],

$$\mu = 2.6693 \times 10^{-5} \frac{\sqrt{MT}}{\sigma^2 \Omega_\mu} \qquad (2)$$

in which $\mu\,[=]\,g\ cm^{-1}\ sec^{-1}$, $T\,[=]\,°K$, $\sigma\,[=]\,Å$ and Ω_μ is a slowly varying function of the dimensionless temperature KT/ϵ [4]. Values of ϵ/K and collision diameter, σ, were calculated from

$$\epsilon/K = 1.15\ T_b, \quad \sigma = 1.166\ (\tilde{V}_b)^{1/3}_{liq} \qquad (3)$$

in which ϵ/K and T_b are in $°K$, $\sigma\,[=]\,Å$, and $\tilde{V}\,[=]\,cm^3\ (g\text{-mole})^{-1}$. For multicomponent gas mixtures, the semi-empirical formula of Wilke [5] was used.

2

$$\mu_{mix} = \sum_{i=1}^{n} \frac{x_i \mu_i}{\sum_{j=1}^{n} x_j \Phi_{ij}} \qquad (4)$$

where

$$\Phi_{ij} = \frac{1}{\sqrt{8}} \left(1 + \frac{M_i}{M_j}\right)^{-1/2} \left[1 + \left(\frac{\mu_i}{\mu_j}\right)^{1/2} \left(\frac{M_j}{M_i}\right)^{1/4}\right]^2 \qquad (5)$$

and n is the number of chemical species in the mixture; x_i and x_j are the mole fractions of species i and j; μ_i μ_j and M_i, M_j are the viscosities and molecular weights respectively.

b. Thermal Conductivity

The Eucken approximation for estimating thermal conductivity of a polyatomic gas at low density was used. [6]

$$k = (C_p + 5/4 \ R) \ \mu/M \qquad (6)$$

where

μ = viscosity
M = molecular weight
R = gas content
C_p = heat capacity.

For a gas mixture (n-components),

$$k_{mix} = \sum_{i=1}^{n} \frac{x_i k_i}{\sum_{j=1}^{n} x_j \Phi_{ij}} \qquad (7)$$

where x_i, x_j and Φ_{ij} are as in equations (4) and (5).

c. Mass Diffusivity

The following formula for the estimation of mass diffusivity of gases at low density was used [7].

3

$$D_{AB} = 0.0018583 \frac{\sqrt{T^3 \left(\frac{1}{M_A} + \frac{1}{M_B} \right)}}{P \, \sigma_{AB}^2 \, \Omega_D} \qquad (8)$$

where

$$\sigma_{AB} = 1/2 \, (\sigma_A + \sigma_B), \qquad (9)$$

$T[=]°K$, M_A, M_B are molecular weights of A and B, $p[=]$atm, $\sigma_{AB}[=]Å$, Ω_D is a dimensionless function of temperature, and $D_{AB}[=]$ cm^2/sec. A summary of transport properties are listed in Table 1.

TABLE 1: ESTIMATED TRANSPORT PROPERTIES

Species	Viscosity μ g cm^{-1} sec^{-1}	Mass Diff. D_{AB} cm^2/sec	Temperature °K	Kinematic Viscosity μ/ρ, cm^2/sec
$CaCl_2$	3.49×10^{-4}		2,073	5.33×10^{-2}
WCl_5	6.20×10^{-4}		2,073	2.91×10^{-2}
$CaCl_2$ WCl_5		(at p = 1.0 atm) 0.37	2,073	
O_2	8.0×10^{-4}		2,073	
CO_2	4.9×10^{-4}		2,073	3.26
CO_2	5.24×10^{-4}		1,598	
H_2	2.65×10^{-4}		1,598	
$ZnCl_2$	5.10×10^{-4}		1,598	
$TiCl_4$	4.60×10^{-4}		1,598	

2. Reactor Gas Mixing

Past experience in the area of gas phase particle production [8] had shown that mixing of reactants was indeed limited. A detailed study of this problem was undertaken to design a reactor which would provide adequate mixing of the reactants and increase the product yield. The example product was $CaWO_4$, produced by the overall reaction.

$$CaCl_2 + WCl_5 + 7/2 \, H_2 + 4CO_2 = 4CO + CaWO_4 + 7HCl \qquad (10)$$
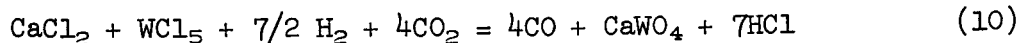
Thermodynamic calculations, previous experience and existing experimental facilities dictated the choice of operating conditions, as well as the reactor configuration. Fluid mechanical and mixing calculations determined the efficiency for the degree of mixing under the chosen operating conditions and reactor configuration.

In Figs. 1 and 2, the proposed reactor configuration is shown. One gas stream is composed of $O_2 + CO_2$, and the other gas stream is composed of $CaCl_2 + WCl_5 + H_2$. Two heat sources were considered: an induction furnace and a oxy-hydrogen flame. A preliminary reactor design was based on stoichiometric reactant flow rates to give a first estimate of reactor dimensions. Heat balance calculations gave information of the additional flow rates of oxy-hydrogen flame. The oxy-hydrogen flame would provide heat for the reaction and create instability and turbulance at the central jet. Revised calculations based on the new rates provided the final reactor configurations and dimensions.

<u>Preliminary Reactor Design</u>: The selected operating conditions were:

Pressure: 0.5 atm
Temperature: 2,074°K
Gas flow rates:
  CO_2 800 cc/min (STP)
  $CaCl_2$ 200 " " "
  WCl_5 200 " " "
  H_2 700 " " "

Stream 1 forms a jet issuing from a 1/2" I.D. tube (central jet) with a volumetric flow rate of $V_1 = 1.2 \times 10^4$ cc/min and an average issuing velocity of $\bar{v}_1 = 1.57 \times 10^4$ cm/sec under the selected operating conditions. Stream 2 is split into eight jets issuing from eight 1/4" orifices (peripheral jets) with a total volumetric flow rate of $V_2 = 1.66 \times 10^4$ cc/min and an average issuing velocity of 1.11×10^2 cm/sec.

The density and kinematic viscosity of Stream 2 was calculated as $P_2 = 2.18 \times 10^{-4}$ g/cc and $v_2 = 1.7$ cm^2/sec respectively; and that of Stream 1 as $P_1 = 1.2 \times 10^{-4}$ gm/cc and $v_1 = 3.26$ cm^2/sec, respectively. Hence the Reynolds numbers of the jets are based on their issuing velocity and diameter.

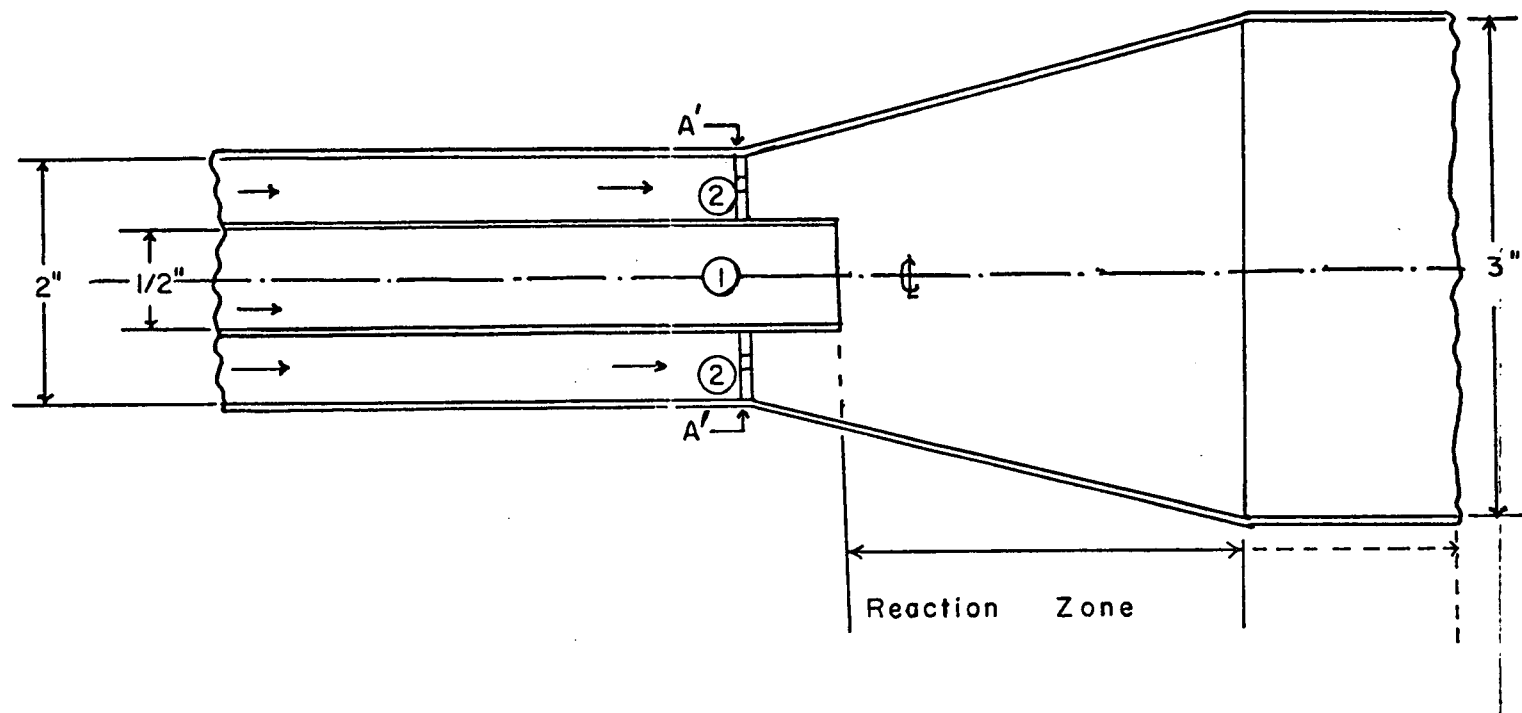$$\text{Central jet:} \quad (N_{Re})_1 = \frac{(157)(1/2 \times 2.54)}{3.26} = 49 \qquad (11)$$
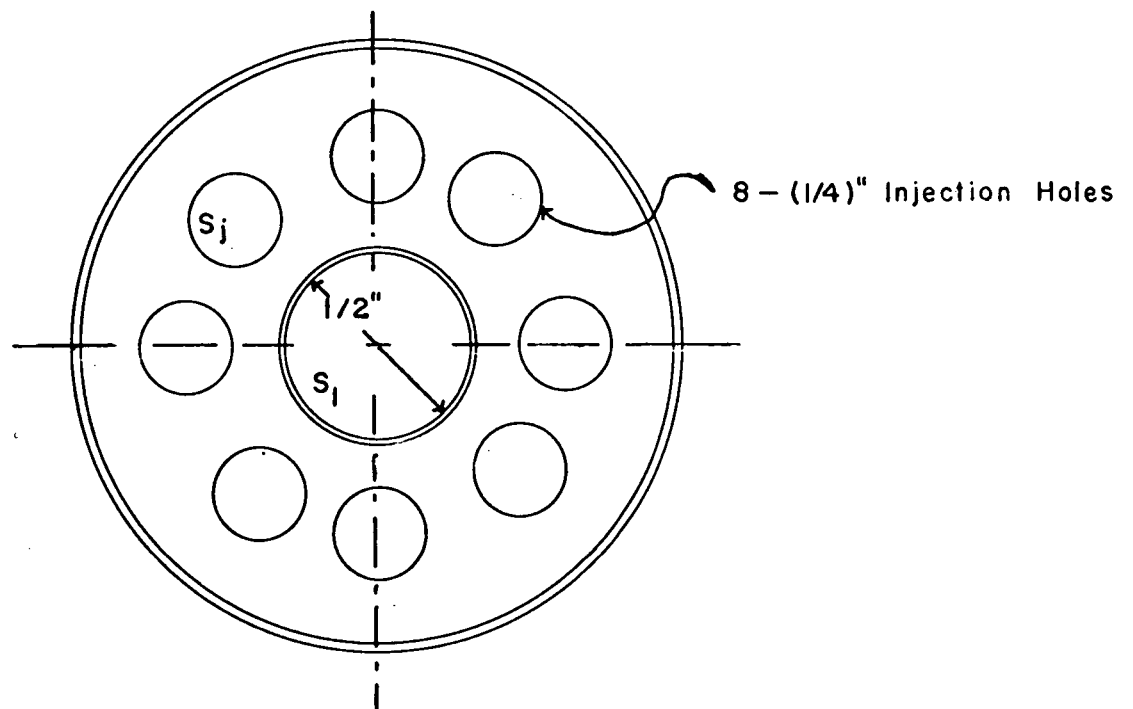
Figure 1. Proposed Reactor Configuration

Figure 2. View A¹A¹ of Figure 1

Peripheral jets: $(N_{Re})_2 = \dfrac{(111) \ (1/4 \times 2.54)}{1.70} = 41$ (12)

Since the transition Reynolds number for a free jet is approximately 30 [9], turbulent velocity fluctuations should be present outside of the jets potential core. Assuming that Stream 1 has fully occupied the cross sectional area of the divergent nozzle of the reactor (Fig. 1); the time (equivalently, the length of the mixing zone) for a prescribed degree of mixing may be determined.

The terminology of mixing may cause confusion, since there is generally a free interchange of words (e.g., blending, mixing, dispersion) and their meanings. Brodkey [10] defines "mixing to mean any blending into one mass and mixture as a complex of two or more ingredients which do not have a fixed proportion to one another and which, however thoroughly comingled, are conceived as retaining a separate existence". The ultimate in any mixing process is submicroscopic homogeneity with molecules uniformly distributed over the field. Molecular diffusion will always be the controlling factor and when it is very slow, turbulence can speed up the diffusion by increasing the transfer area. It is the dispersive action inherent in turbulence that enhances the molecular diffusion.

Criteria characterizing the quality of mixing are defined for the purpose of this report [17]; their mathematical treatments are available elsewhere. [10-17]

Scale of segregation: A measure of the size of the unmixed clumps of the pure components. As these clumps are dispersed, the scale of mixing is reduced. A linear scale, L_S, is defined as

$$L_S = \int g_S(r) \ d\vec{r} \qquad (13)$$

where,

$$g_S(r) = \dfrac{\overline{a(\vec{x}) \ a \ (\vec{x} + \vec{r})}}{a'^2} \qquad (14)$$

and

$a = c - \bar{c}$ = concentration fluctuation
c = instantaneous concentration
$\bar{c}$ = time-average concentration
a' = rms fluctuation $\equiv \sqrt{\overline{a^2}}$.

8

A volume scale, V_s, is defined as

$$V_s = \int 2\pi \, \vec{r}^2 g_s(r) \, d\vec{r} \tag{15}$$

where $\vec{x}$ and $\vec{r}$ are vector distances and $r = \left| \vec{r} \right|$.

Intensity of segregation: The effect of molecular diffusion on the mixing process is a measure of the difference in concentration between neighboring clumps of fluid. The intensity of segregation is defined as

$$I_s = \frac{a'^2}{a'^2_o} \tag{16}$$

The intensity of segregation is unity for complete non-mixing and equal to zero when the mixture is perfectly uniform ($a'^2 = 0$). Figure 4 is a schematic representation of the scale and intensity of segregation during a gas mixing process. [18]

The statistical theory of turbulence suggests the following relations

$$I_s = e^{-t/\tau} \tag{17}$$

where

$\quad$ t = time of mixing

$\quad$ τ = time constant

$$\tau = 1/2 \left[3 \left(\frac{5}{\pi} \right)^{2/3} \left(\frac{L_s}{\epsilon} \right)^{1/3} + \left(\frac{\upsilon}{\epsilon} \right)^{1/2} \cdot \ln N_{sc} \right] \tag{18}$$

and

$\quad$ υ $\quad$ = kinematic viscosity = $\mu/\rho \, [=] cm^2/sec$
$\quad$ N_{sc} = Schmidt number = υ/D
$\quad$ D $\quad$ = molecular mass diffusivity $[=] cm^2/sec$
$\quad$ L_s $\quad$ = scale of segregation

The scale of segregation, L_s, can be estimated.

$$\left(\frac{5}{\pi} \right)^{2/3} \left(\frac{L_s}{\epsilon} \right)^{1/3} = \frac{\lambda^2}{10\upsilon} = \frac{0.341 \, r_o}{\mu'} \tag{19}$$
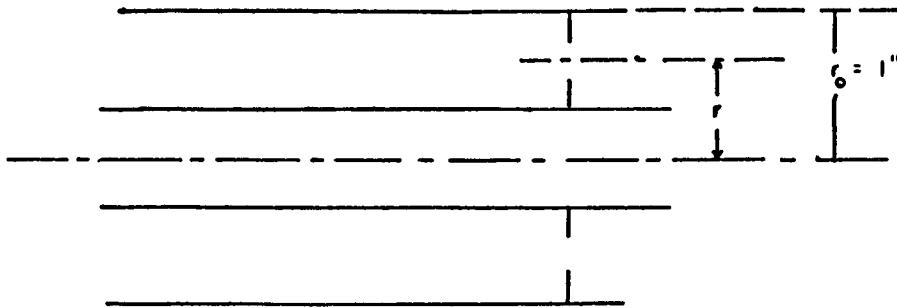
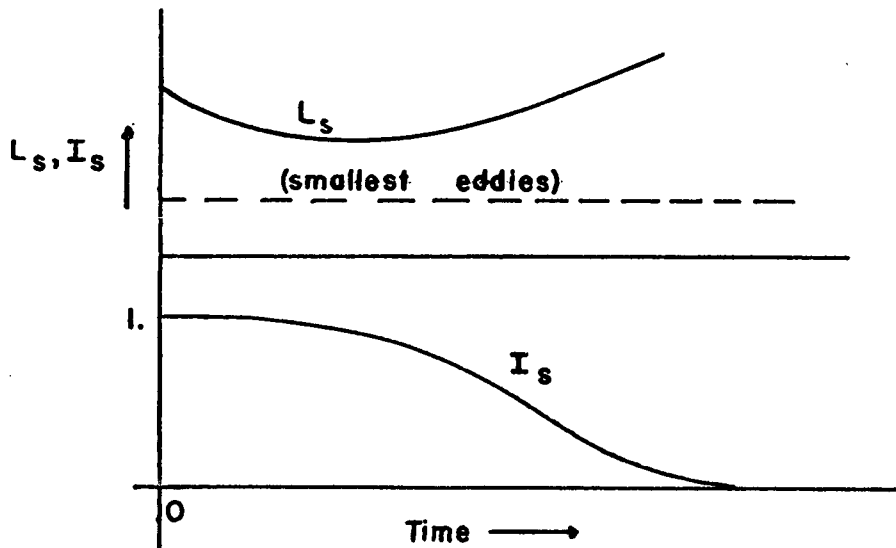Figure 3. Geometry Used for Mixing Calculations

Figure 4. The Intensity and Scale of Segregation
During Mixing (18)

$$\lambda^2 = 15 \upsilon \, u'^2 / \epsilon \tag{20}$$

where

λ = a microscale of mixing

$u' = \sqrt{\overline{u^2}}$ = rms velocity fluctuation in the axial direction

In summary, the key to the mixing is the determination of the time constant, τ. From equation (17), the time of mixing may be calculated for any desired value of the intensity of segregation I_s, i.e., degree of mixing.

Mixing Calculations

Values of the intensity of segregation were calculated for different values of the rms value of the axial velocity fluctuation, u'. The geometry is shown in Figs. 1-3.

Two cases were considered:

(a) <u>Mixing of the peripheral jets (1/4" nozzle) with surrounding gas considered as stagnant.</u> Three values of u' were assumed; $u_1 = 0.05\bar{v}_2$, $u_2 = 0.025\bar{v}_2$ and $u_3 = 0.01\bar{v}_2$, where $\bar{v}_2 = 110$ cm/sec. Corresponding time constants were calculated: $\tau_1 = 0.236$ sec, $\tau_2 = 0.472$ sec, and $\tau_3 = 1.165$. Figure 5 summarizes the results of this case where the intensity of segregation is plotted against time.

(b) <u>Mixing of the central jet with surrounding gas considered stagnant.</u> Time constants of mixing were calculated as in the preceeding case with $\bar{v}_1 = 157$ cm/sec. The corresponding time constants were calculated as: $\tau_1 = 0.110$ sec, $\tau_2 = 0.332$ sec and $\tau_3 = 0.830$ sec. Figure 6 summarizes the results of this case.

The length of the reaction zone was calculated on the basis of mixing time (for a given intensity of segregation and an average flow velocity of both gas streams). For an 80% degree of mixing, i.e., $I_s = 0.2$, and an average gas velocity of 23.5 cm/sec the time of mixing was calculated as $t = 1.875$ sec. Taking $N = 2$[*], the dimensionless measure of mixing distance, σ,

$$\sigma = k_0 u' t \tag{21}$$

drops from $\sigma = 6$ to $\sigma \cong 4.5$[*]. Hence the actual mixing time is

$$t_{mix} = 1.875 \left(\frac{4.5}{6}\right) \cong 1.40 \text{ sec} \tag{22}$$

[*][20]

11
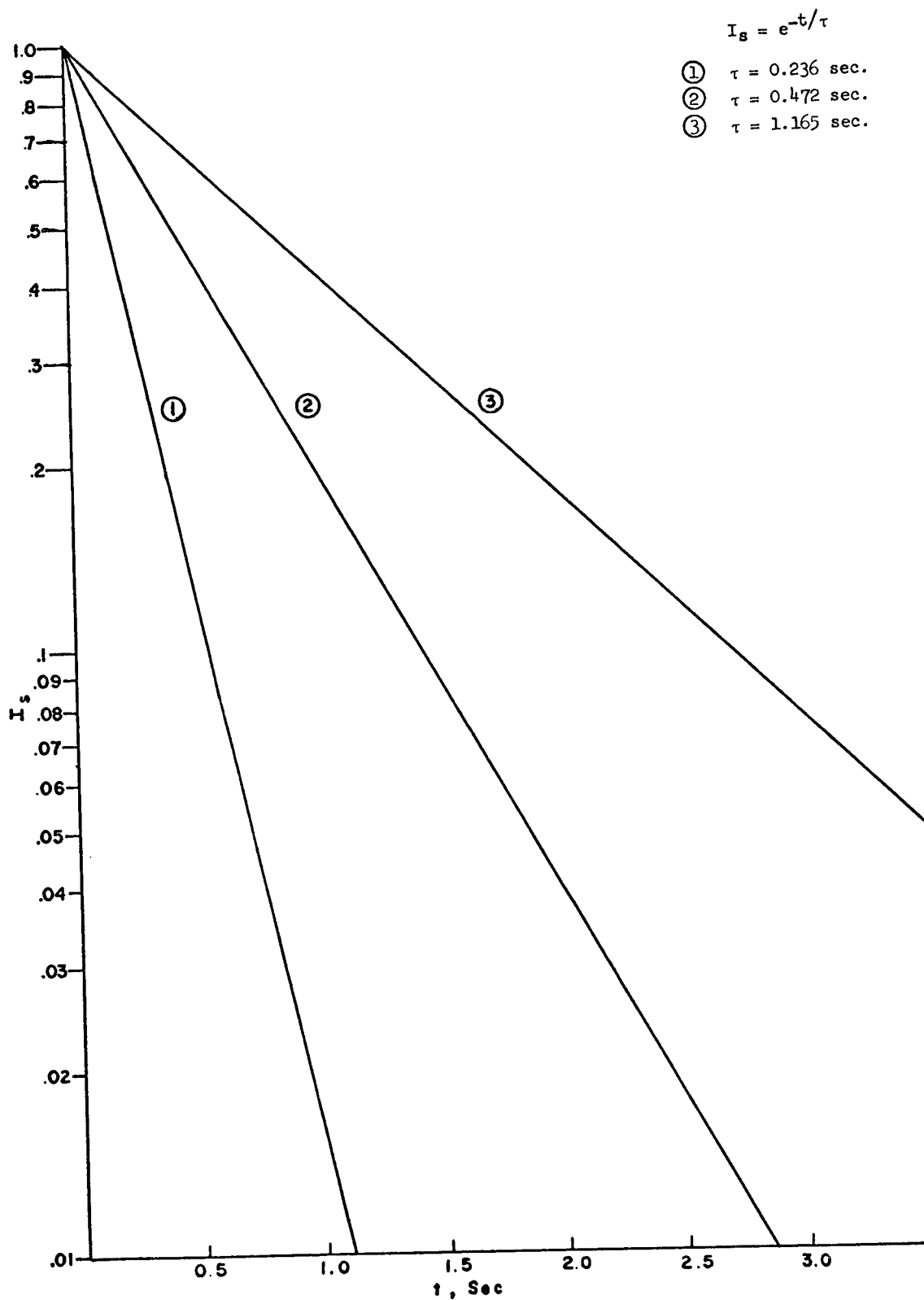
Figure 5.   Preliminary Reactor Design.   Mixing of
Stream 2

12
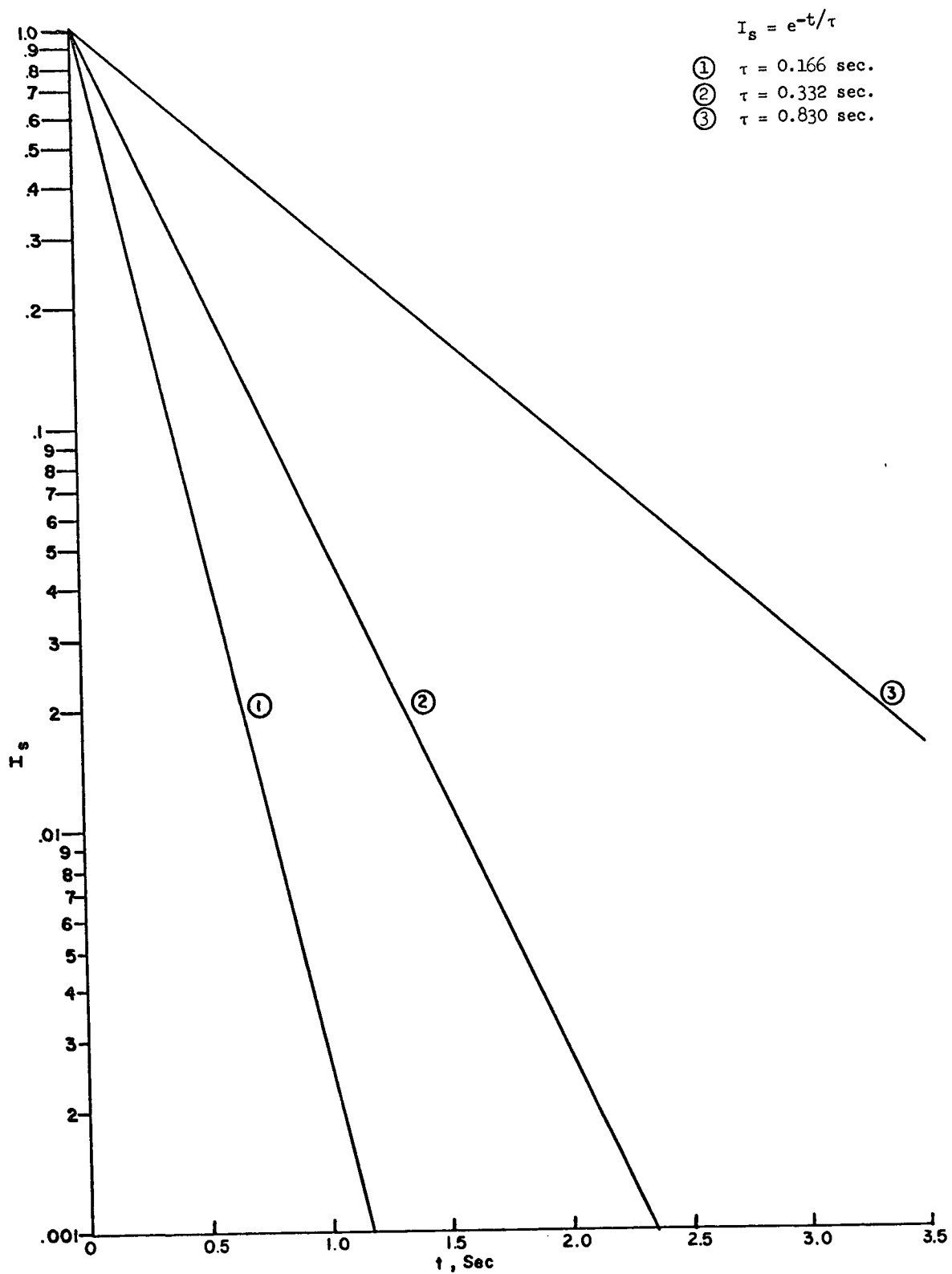
Figure 6. Preliminary Reactor Design. Mixing of Stream 1

The graph shows $I_s = e^{-t/\tau}$ plotted on a semi-log scale with I_s on the vertical axis (ranging from .001 to 1.0) and t, Sec on the horizontal axis (ranging from 0 to 3.5).

① $\tau = 0.166$ sec.
② $\tau = 0.332$ sec.
③ $\tau = 0.830$ sec.

13

and the length of the mixing zone

$$L_m = (23.4 \text{ cm/sec}) (1.4 \text{ sec}) \cong 32.8 \text{ cm} \quad . \tag{23}$$

These preliminary reactor design data formed the basis for subsequent reactor design.

Reactor Design

The rms value of the axial velocity fluctuation, u', varies with distance downstream in the reactor. Moreover due to the spreading of the central and peripheral jets, their average velocity also varies with distance downstream in the reactor. The spreading of the jets is not free, due to interactions of two adjacent peripheral jets and the central jet. Thus, the flow field becomes extremely complicated and almost hopeless from an exact analytical point of view.

Semi-empirical approximations have been used as well as reasonable simplifications to make the problem tenable. An energy (heat) balance around the reactor established the heat requirements being supplied by the oxy-hydrogen flame, thus revising the flow rates in the central jet.

There is a wealth of information concerning free turbulence and especially round free jets. [21-23] Figures 7 and 8 show the nomenclature and configurations used in these calculations.

The jet issues with a velocity v_p from an orifice with diameter, d, into a stream with uniform velocity v_s. In the jet region, the axial velocity component $\overline{v}_x$ is assumed to be composed of the velocity v_s of the ambient stream and the velocity $\overline{v}_1$, which is the deviation from the velocity v_s caused by the jet (Fig. 7). Close to the orifice, the turbulent mixing zone has zero width W; this width W(x) increases with increasing distance from the orifice to a distance x_c where the mixing zone covers the entire jet (Fig. 8). If the velocity distribution at the orifice is uniform, the velocity at the axis maintains its constant value v_p up to this distance x_c. Up to x_c, the jet contains a central potential cove region. Farther downstream the velocity at the axis of the jet decreases with increasing distance.

The length of the core region, x_c, is determined mainly by the value of the ratio $\mu \equiv v_s/v_p$; one empirical correlation [24] is:

$$\frac{x_c}{d} = 4 + 12\mu \tag{24}$$

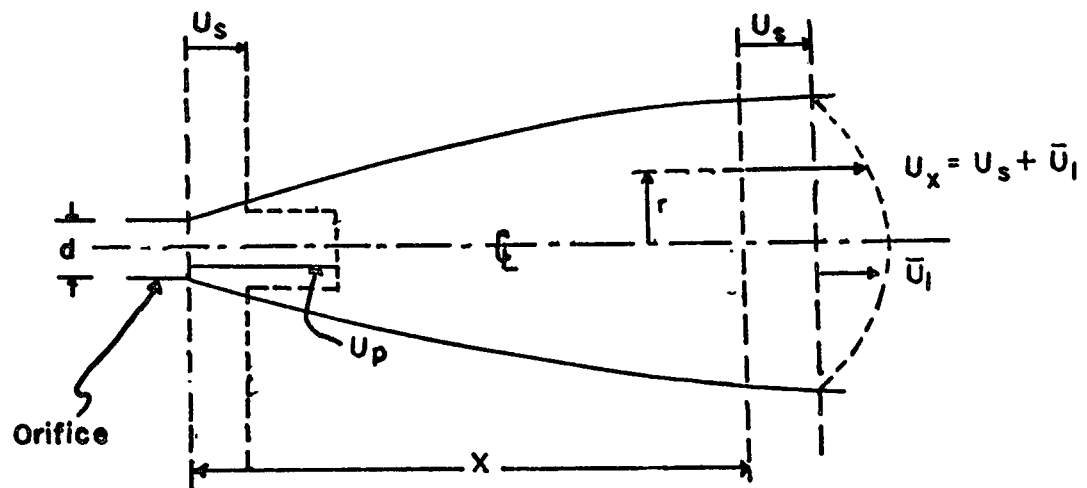The velocity of the jet at the axis decreases hyperbolical with increasing downstream distance x,
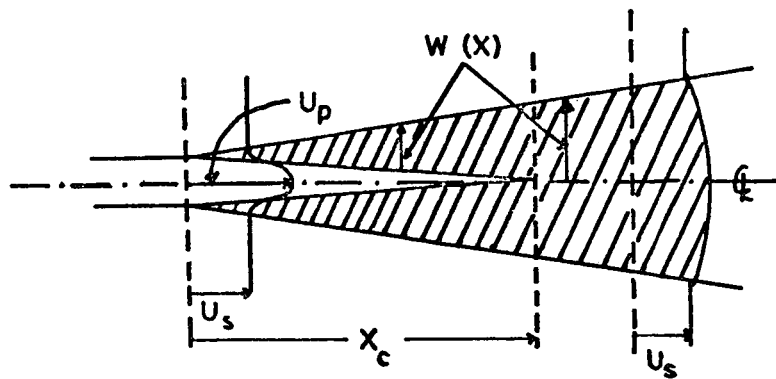
Figure 7. Geometry Nomenclature for Round Jet

Figure 8. Geometry for Round Jet

$$\frac{\overline{v_1}_{,max}}{v_p - v_s} = \frac{x_c}{x} \text{ for } x > x_c \qquad (25)$$

and the change in jet width, W, is given by

$$\frac{W}{d} = \left(\frac{x}{\mu}\right)^{1-\mu} \text{ for } x > x_c \quad . \qquad (26)$$

The heat of reaction of the oxy-hydrogen flame was calculated as: -60.298 Kcal/g-mole at $T = 2,073°K$. From the heat balance calculations around the reactor it was determined that the amount of heat supplied by the oxy-hydrogen flame is

$$Q_f = 40 \text{ Kcal/hr} \qquad (27)$$

Hence the volumetric flow rates were revised.

$$V_1 = 1.373 \times 10^4 \text{ cc/min} \qquad (28)$$
$$(T = 2,073°K, \ p = 0.5 \text{ atm})$$
$$V_2 = 2.005 \times 10^4 \text{ cc/min} \qquad (29)$$

and the corresponding Reynolds numbers were calculated to be

$$N_{Re_1} = 56.2; \ N_{Re_2} = 37 \qquad (30)$$

Under these new flow conditions v_p for the central jet was calculated as $v_p = 179.5$ cm/sec. Since $\mu = v_s/v_p$ and downstream interaction between central and peripheral jets occurs, it is obvious that μ depends on x. An average value of μ was estimated on the basis of two limiting values of $v_s = 17.6$ cm/sec and $v_s = 134$ cm/sec; for $\mu_{Avg} = 0.223$ the total velocity at the centerline, $(\overline{v_x})_o = \overline{v_1} + v_s$, was calculated as

$$(\overline{v_x})_o = \frac{1,180}{x} + 40 \qquad (31)$$

and the jet width as

$$W = 0.24 \ (x)^{0.777} \qquad (32)$$

where $(\overline{v_x})_o$ [=] cm/sec; x, w, [=] cm. The results are shown in Fig. 9. Similar calculations for the peripheral jets and available data [25], gave $x_c = 8.5$ cm, $\mu = 0.61$
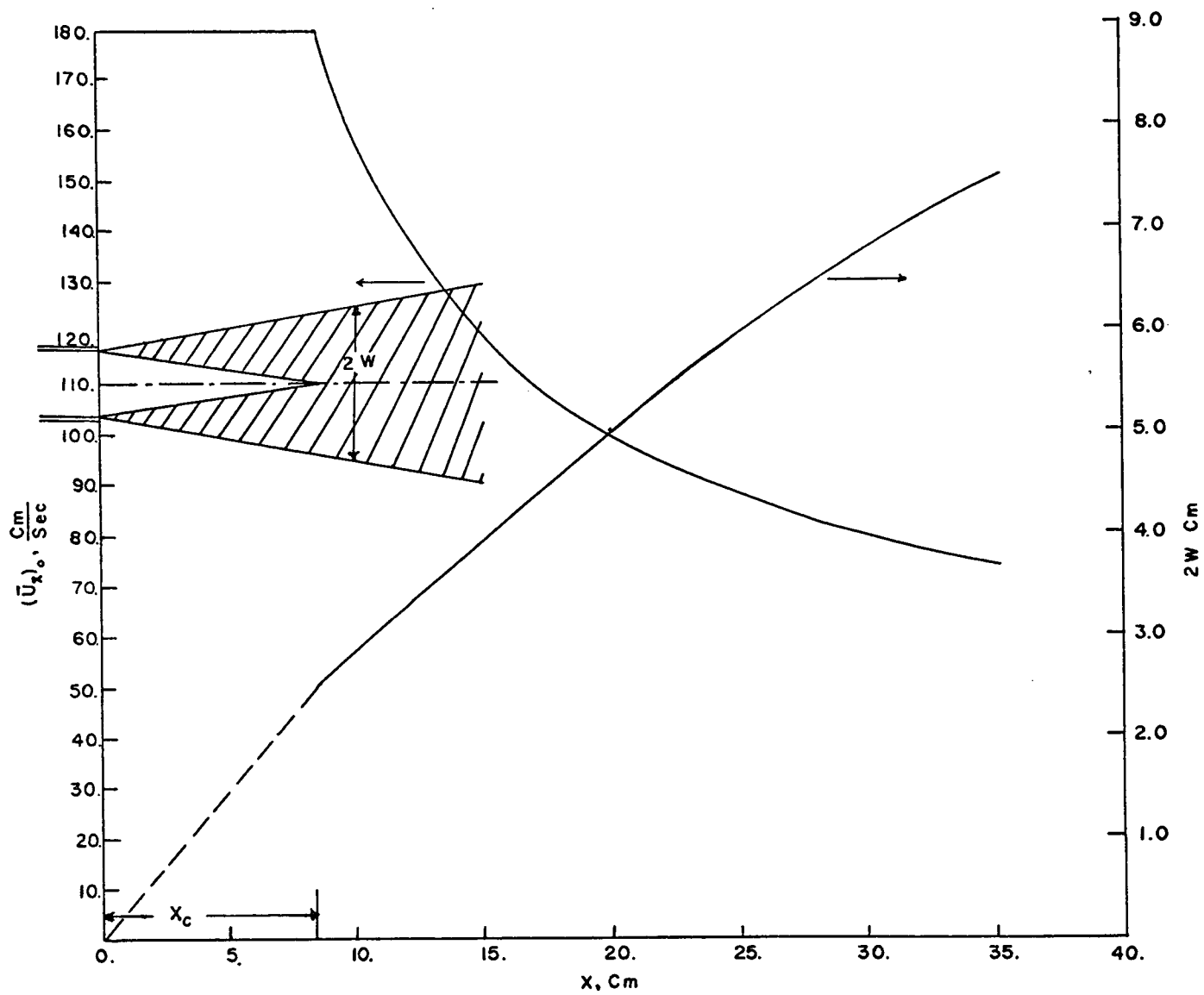
Figure 9. Velocity at the Center Line and Width
Variation for Downstream of Central Jet

17

and

$$(\bar{v}_x)_o = \frac{374}{x} + 82 \qquad (33)$$

$$W = 0.294 \ (x)^{0.39} \ . \qquad (34)$$

The results are shown in Fig. 10. The rms value u' was calculated using available data [26]. For the central jet and at a radial distance of r = 1 cm,

$$u' = \frac{1.8 \times 10^2}{(x - 1.02)} \sqrt{g_1 \left(\frac{r}{x - 1.02}\right)}; \ [=] \ cm/sec \qquad (35)$$

where x[=]cm, and the function g was obtained from reference [27]. Since those data were for much higher jet Reynolds number, the predicted values of u' from equation [31] are rather high. Due to lack of other data this calculation was retained for comparison. Hinze [28] gives the following correlation for the axial (x-direction) eddy viscosity, $(\epsilon_m)_{xx}$.

$$(\epsilon_m)_{xx} = 0.013 \ v_p d; \ [=] \ cm^2/sec \qquad (36)$$

where v_p [=] cm/sec and d [=] cm.

The corresponding Reynolds (eddy) stresses are given by the well known expression

$$\overline{\mu_x \mu_x} = -(\epsilon_m)_{xx} \frac{dv}{dx} \qquad (37)$$

Using Figs. 9 and 10 or equations (27) and (29), the velocity gradients at the centerline may be calculated. The following experssions for u' for both the central and peripheral jets can be obtained.

$$\text{Central jet:} \quad u' = \frac{59}{x} \qquad (38)$$

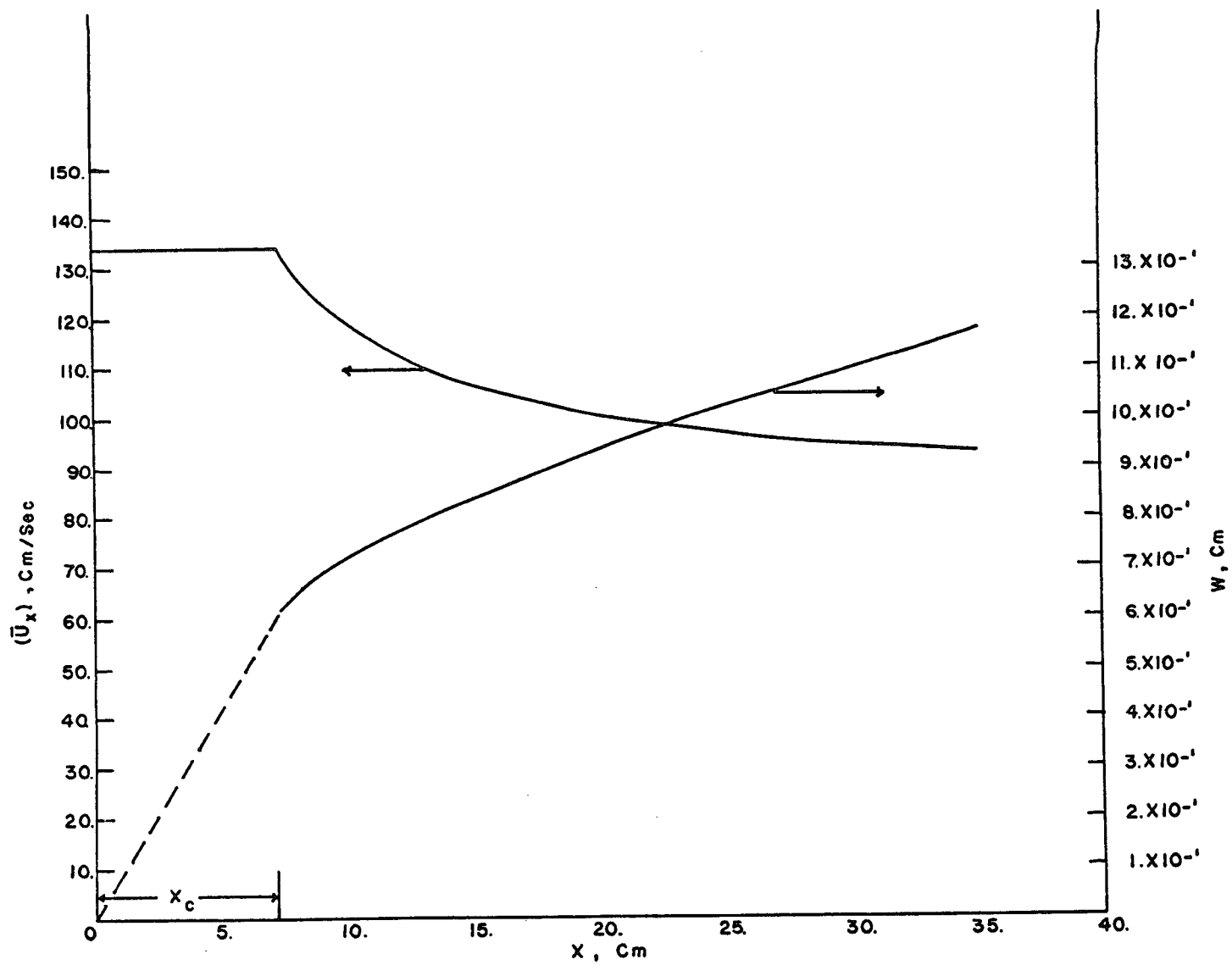$$\text{Peripheral jets:} \quad u' = \frac{20.3}{x} \qquad (39)$$

Figure 10. Peripheral Jets

where $x[=]$cm, $u'[=]$cm/sec. These results are summarized in Fig. 11. It is worth noticing that u' for the peripheral jets is lower than for the central jet. Half way in the x-direction of a ~35 cm long reaction zone, $u' \simeq 1.3$ cm/sec; the velocity $(\bar{v}_x)_0$ at the same x is 100 cm/sec [Fig. 10] or $u' \simeq 0.013 \ (v_x)_0$.

From Fig. 11, one may graphically calculate a reactor length for a chosen intensity of segregation. Additionally, an analytic solution was attempted. For gases, with the Schmidt number very close to unity, equations (18) and (19) give for the time constant, τ,

$$\tau = \frac{3}{2} \left(\frac{0.341 \ r_0}{u'} \right) \tag{40}$$

for $r_0 = 1$ inch $= 2.54$ cm, and for the central jet (equation 3) $\tau = 0.022 \ x$, $x \ [=]$ cm and $\tau \ [=]$ sec. The intensity of segregation becomes

$$I_s(x,t) = \exp \left[-\frac{t}{0.022x} \right] . \tag{41}$$

The total volumetric flow rate (Streams 1 and 2) was

$$V = 1.373 \times 10^4 + 2.005 \times 10^4 = 3.378 \times 10^4 \ \text{cc/min} = 5.62 \times 10^2 \ \text{cc/sec} \tag{42}$$

From the geometry shown in Fig. 12, it is easily seen that $R = 2.54 + (1.27/L)x \ [=]$ cm. If $v = v(x)$ is the average velocity based on the total cross sectional area,

$$v(x) = \frac{dx}{dt} = \frac{V \ [=] \ \text{cc/sec}}{\pi R^2} = \frac{562}{\pi \left(2.54 + \frac{1.27}{L} x \right)^2} \tag{43}$$

If $L = 35$ cm, equation (43) represents the intensity of segregation as

$$I_s(x) = \exp \left[-0.279 \ (4.4 \cdot 10^{-3}x^2 + 9.2 \cdot 10^{-2}x + 6.45) \right] \equiv e^{-\psi} \tag{44}$$

where $x[=]$cm and $8.9 < x < 35$. Table 2 lists the values of $I_s(x)$ from equation (44).
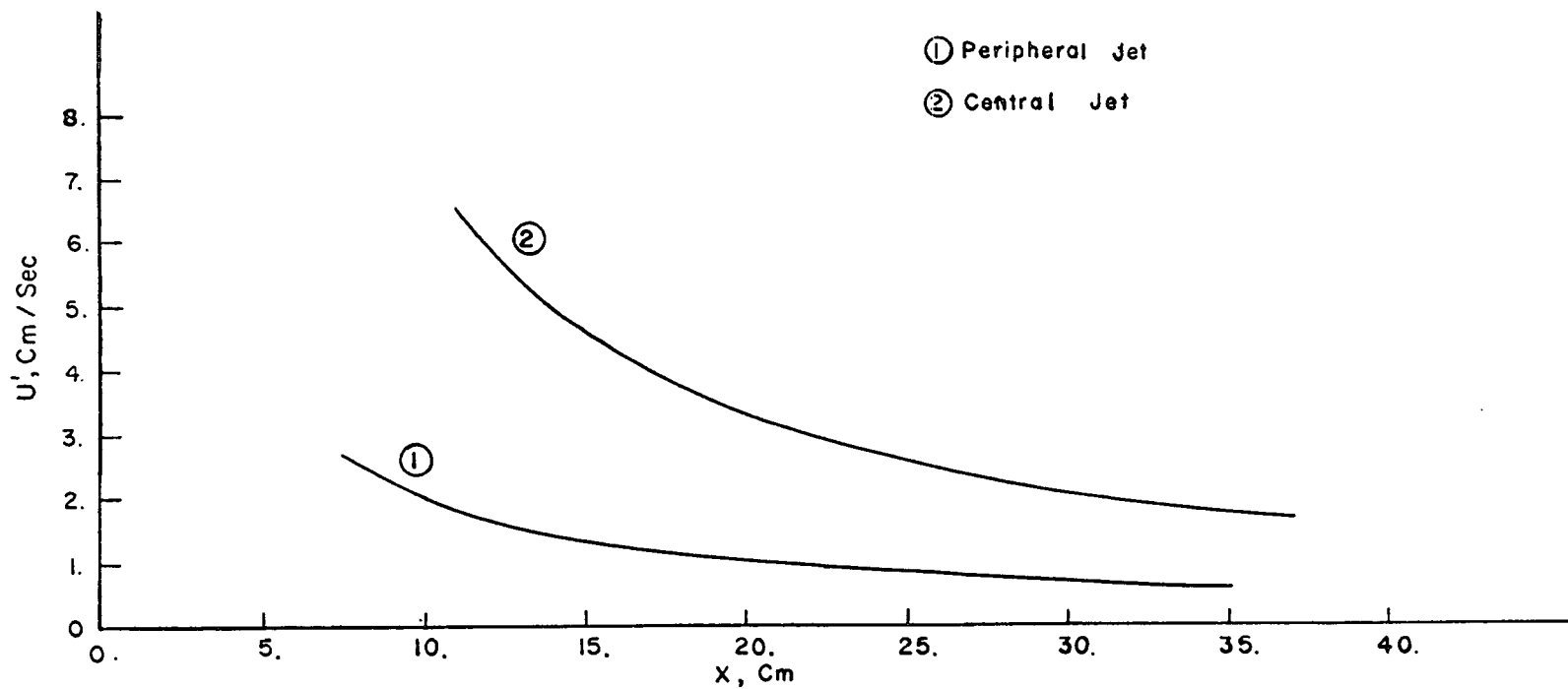
Figure 11.   Variation of Axial Turbulence Intensity
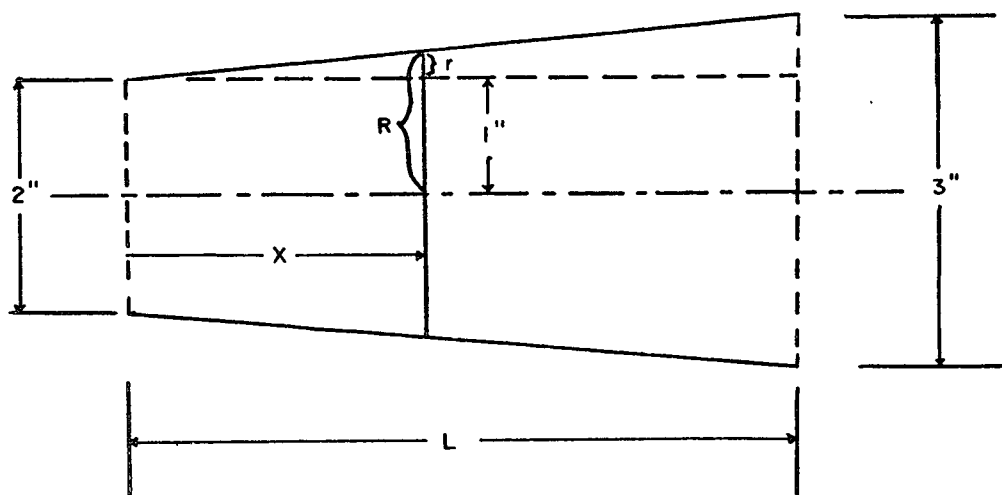Along the Jet Center Line with X

21

Figure 12. Geometry for Calculating Residence Time in Reactor

TABLE 2: INTENSITY OF SEGREGA-
TION FROM EQUATION (44)

x[=]cm	ψ	$I_s = e^{-\psi}$
9	2.13	0.119
10	2.16	0.115
15	2.47	0.094
20	2.78	0.072
25	3.21	0.040
30	3.77	0.023
35	4.20	0.016

It is obvious from Table 2, that the calculation of time based on the total cross-sectional area gives high values for t, thus decreasing the intensity of segregation very rapidly.

Recent research [29] in gas jet mixing suggested that the length of the potential core $x_c \simeq L_s \simeq r_0$, at least for the initial period of mixing i.e., for $0 < x < x_c$. A conservative calculation performed on this basis resulted in the following. For the central jet and $0 < x < x_c = 8.9$ cm, $r_0 \simeq x_c$, u' $\simeq$ 7 cm/sec, the u' close to the end of the potential core [Fig. 11], the time constant, τ, was calculated.

$$\tau = \frac{(0.341)\ (8.9\ cm)}{7\ cm/sec} = 0.434\ sec \tag{45}$$

For the region: $8.9 < x < 35$ cm, $r_0 \simeq 2.5$ inches = average of the two diameters of 2" and 3". u' $\simeq$ 2 cm/sec (i.e., u' at the end of the reaction zone)

$$\tau = \frac{(0.341)\ (6.35\ cm)}{2\ cm/sec} = 1.07\ sec \tag{46}$$

The results for the intensity of segregation and time are shown in Fig. 13. A time for the central jet to travel the total length of the reactor was calculated.
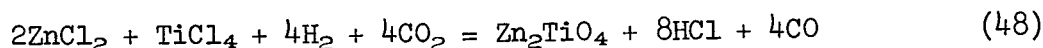
$$t = \frac{8.9\ cm}{179\ cm/sec} + \frac{(35-8.9)\ cm}{93\ cm/sec} = 0.33\ sec \tag{47}$$

(see Fig. 9)

The corresponding intensity of segregation from Fig. 13 was $I_S \cong 0.66$, or 34% mixing.

3. Reactor Mixing for Zn_2TiO_4

The proposed $CaWO_4$ reactor mixing performance is estimated for the production on Zn_2TiO_4 according to the reaction:

$$2ZnCl_2 + TiCl_4 + 4H_2 + 4CO_2 = Zn_2TiO_4 + 8HCl + 4CO \qquad (48)$$

The reactor configuration, gas flow rates, operating temperature and pressure are given in Fig. 14. The amounts of O_2 and H_2 in stream (1) are the ones for the oxy-hydrogen flame and for the purpose of this estimation they were based on a heat supply of 40 kcal/hr by the oxy-hydrogen flame.

Gas flow rates

Stream (1):

$ZnCl_2$	400	cc/min	(STP)
H_2	248	"	"
CO_2	400	"	"
O_2	124	"	"

Stream (2):

$TiCl_4$	200	cc/min	(STP)
H_2	800	"	"

Temperature: 1,300°C
Pressure: 0.5 atm.

The volumetric flow rates of streams (1) and (2) at 1,300°C and 0.5 cc/min were calculated as:

$$V_1 = (1,172) \times \left(\frac{1}{0.5}\right)\left(\frac{1,598}{298}\right) \cong 12,480 \text{ cc/min} \qquad (49)$$

$$V_2 = (1,000) \times \left(\frac{1}{0.5}\right)\left(\frac{1,598}{298}\right) \cong 10,700 \text{ cc/min} \qquad (50)$$

The corresponding velocities of the central jet, $\bar{v}_1$, and each of the eight peripheral jets were calculated (at the operating temperature and pressure)
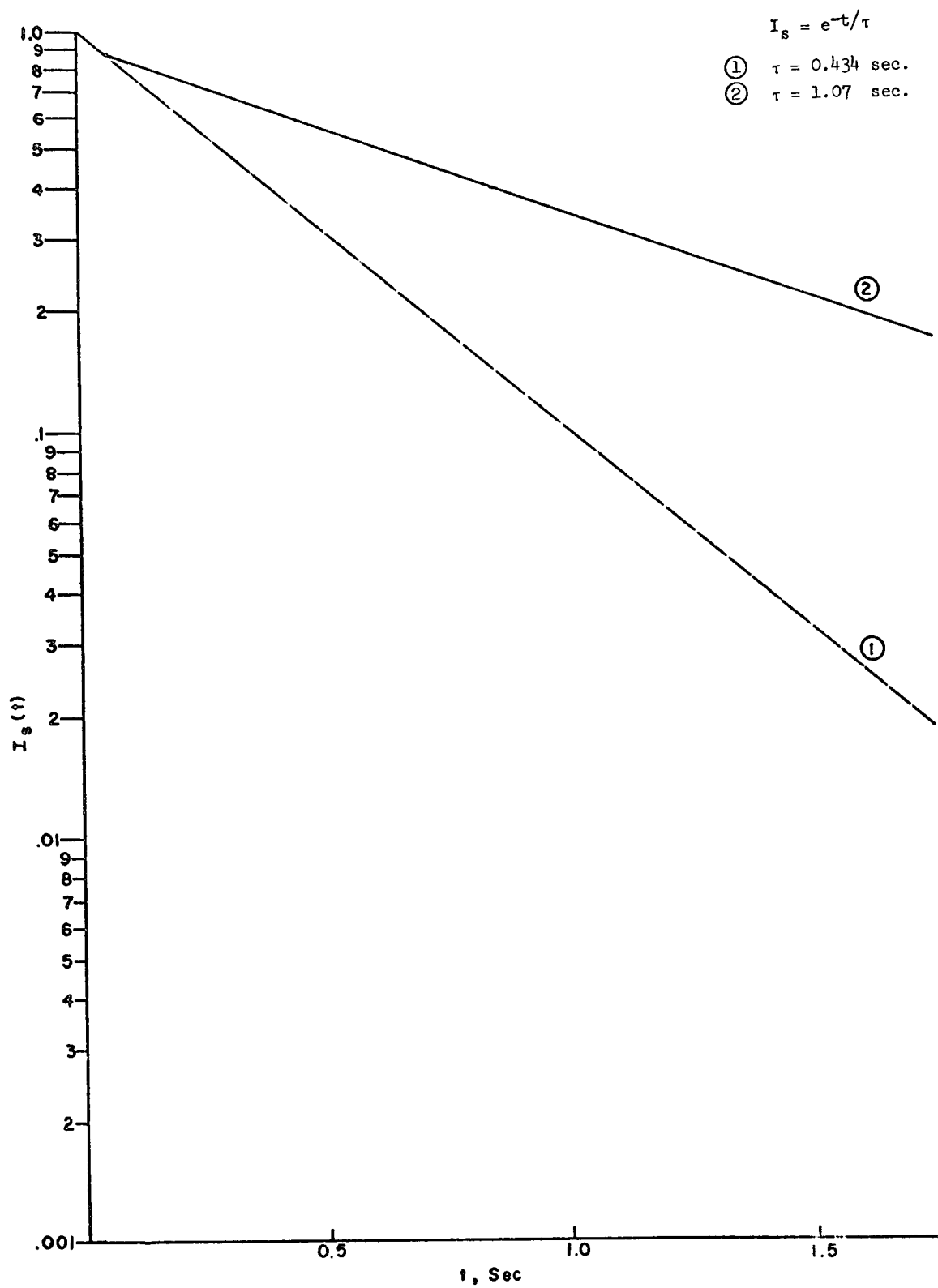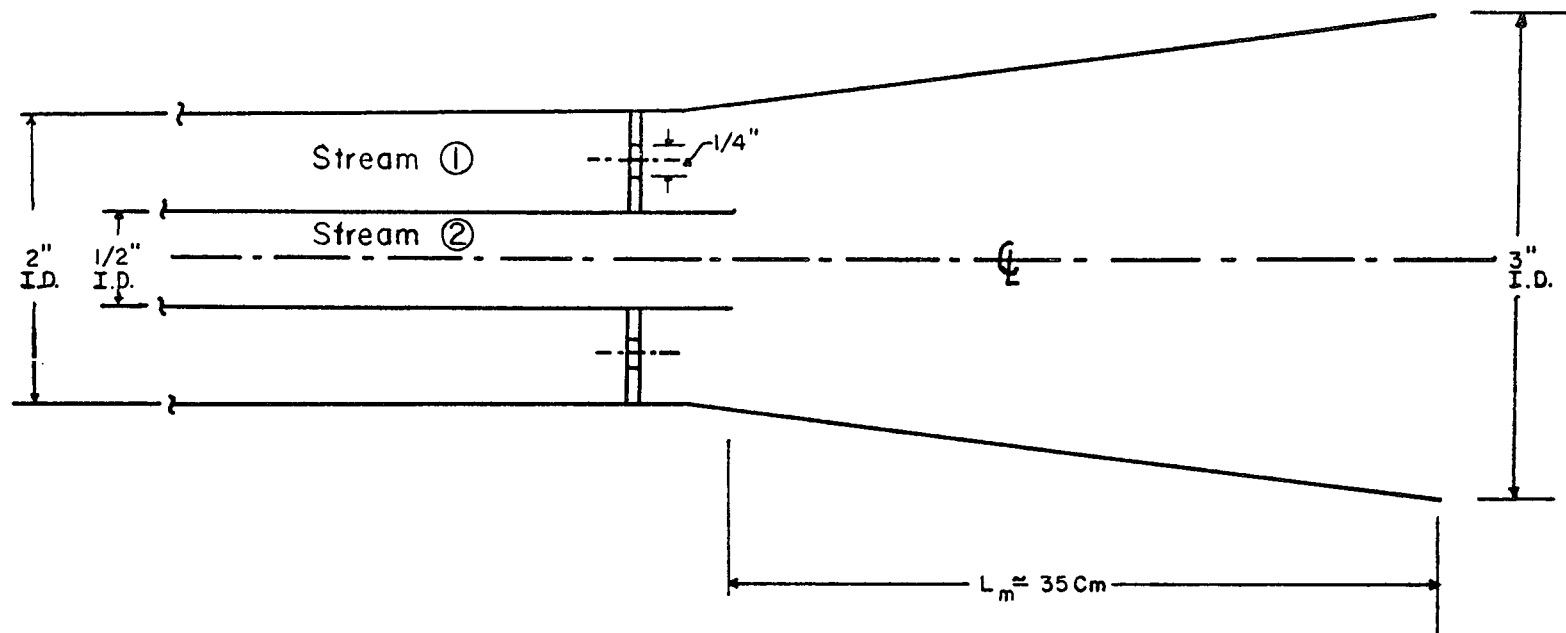
Figure 13. Mixing of Central Jet

25

Stream ①

1/4"

Stream ②

2"
I.D.

1/2"
I.D.

3"
I.D.

$L_m \cong 35 \, Cm$

Figure 14.   Reactor Configuration for the Production
of Zn_2TiO_4

$$\bar{v}_1 = \frac{(12,480 \text{ cc/min})}{(2.53 \text{ cm}^2)(60 \text{ sec/min})} = 82.3 \text{ cm/sec} \tag{51}$$

$$\bar{v}_2 = \frac{(8,460)}{(0.315)(60)(8)} = 5.60 \text{ cm/sec} \tag{52}$$

The kinematic viscosities of streams (1) and (2) were estimated as $v_1 = 1.77 \text{ cm}^2/\text{sec}$ and $v_2 = 1.38 \text{ cm}^2/\text{sec}$ (see Table 1) respectively. The corresponding Reynolds number of the central jet was calculated as $N_{Re} = 59$.

Jet mixing estimation

Equation (24) with a ratio of velocities $\mu = v_s/v_p = 56/82 = 0.68$, gives for the length x_c of the central jet core region.

$$x_c = (4 + 12 \times 0.68) \times (1.27) = 15.4 \text{ cm} \tag{53}$$

The velocity at the centerline of the jet $(\bar{v}_x)_o$ was calculated from equation (25) as:

$$\frac{(\bar{v}_x)_o - v_s}{v_p - v_s} = \frac{x_c}{x}$$

or

$$(\bar{v}_x)_o = \frac{400}{x} + 56; \quad x[=]\text{cm}, \quad (\bar{v}_x)_o[=]\text{cm/sec} \tag{54}$$

Equation (36) for the eddy viscosity $(\epsilon_m)_{xx}$ gave:

$$(\epsilon_m)_{xx} = (0.013)(82)(1.27) \cong 1.36 \text{ cm}^2/\text{sec} \tag{55}$$

From equation (54),

$$\frac{d(v_x)_o}{dx} = -\frac{400}{x} \tag{56}$$

which combined with equ. (55) reduced equ. (31) to:

$$u' = \sqrt{+ (1.36)\frac{400}{x^2}} = \frac{23.4}{x} \quad [=]\text{cm/sec}; \quad x[=]\text{cm} \tag{57}$$

The time constant of mixing, τ, was calculated from equations (18) and (19) at a radial distance $r_0 = 1$ in.,

$$\tau = \frac{1}{2} \times \left[3 \times \frac{(0.341)\ (2.54)}{1.4} \right] = 0.93 \text{ sec} \qquad (58)$$

The intensity of segregation

$$I_s = e^{-t/0.93}, \quad t[=]\text{sec} \qquad (59)$$

is plotted vs mixing time in Fig. (15). At a downstream distance $x = 20$ cm the velocity at the centerline of the central jet is: $(\overline{v}_x)_0 = 76$ cm/sec (from equation 54). This velocity was used to calculate a residence time in the reactor. This is a conservative estimate as far as mixing because the jet velocity drops continuously downstream, and the central jet is the faster one; in addition the velocity profile has its maximum at the center line of the jet reaching the value $v_s = 56$ cm/sec at the most, towards the boundaries of the expanding nozzle of the reactor. A mixing time based on the $L_m \simeq 35$ cm reactor length and the volume velocity was calculated as $t = (35 \text{ cm})/(76 \text{ cm/sec}) \simeq 0.46$ sec, giving $I_s \cong 0.60$ for the intensity of segregation, i.e., 40% mixing. Hence, even this conservation estimate gives an adequate degree of reactants mixing in the case of Zn_2TiO_4 production.

B. Equipment Design and Modification

A silicon carbide tube furnace was modified to incorporate the reactor design based on the mixing studies, Fig. 16. Temperature capability was extended beyond 1800°C with a high frequency induction furnace utilizing the improved reactor design, Fig. 17. This reactor provides the localized induction heating and adequate mixing of the reactant gases.
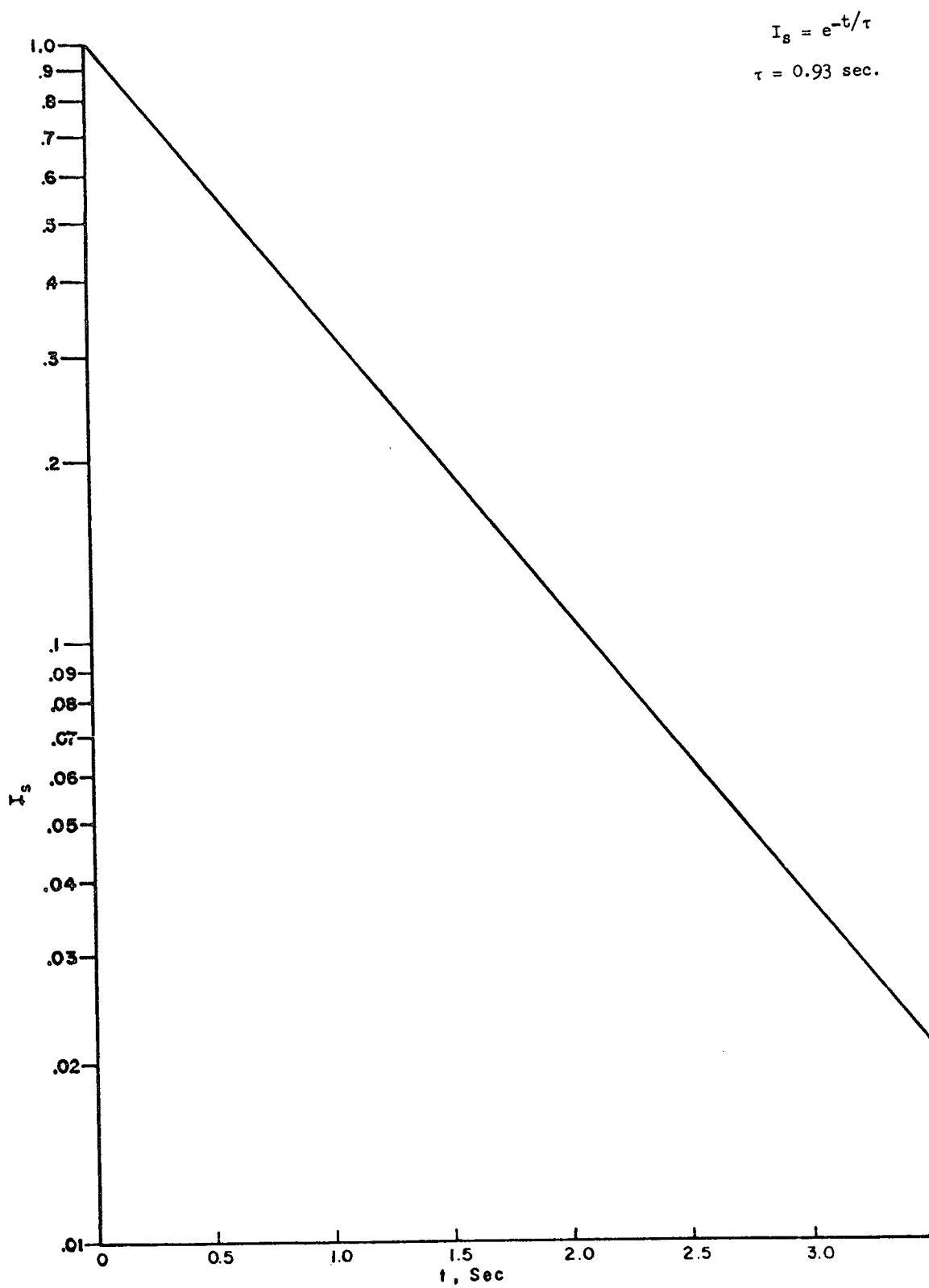
$$I_s = e^{-t/\tau}$$

$$\tau = 0.93 \text{ sec.}$$

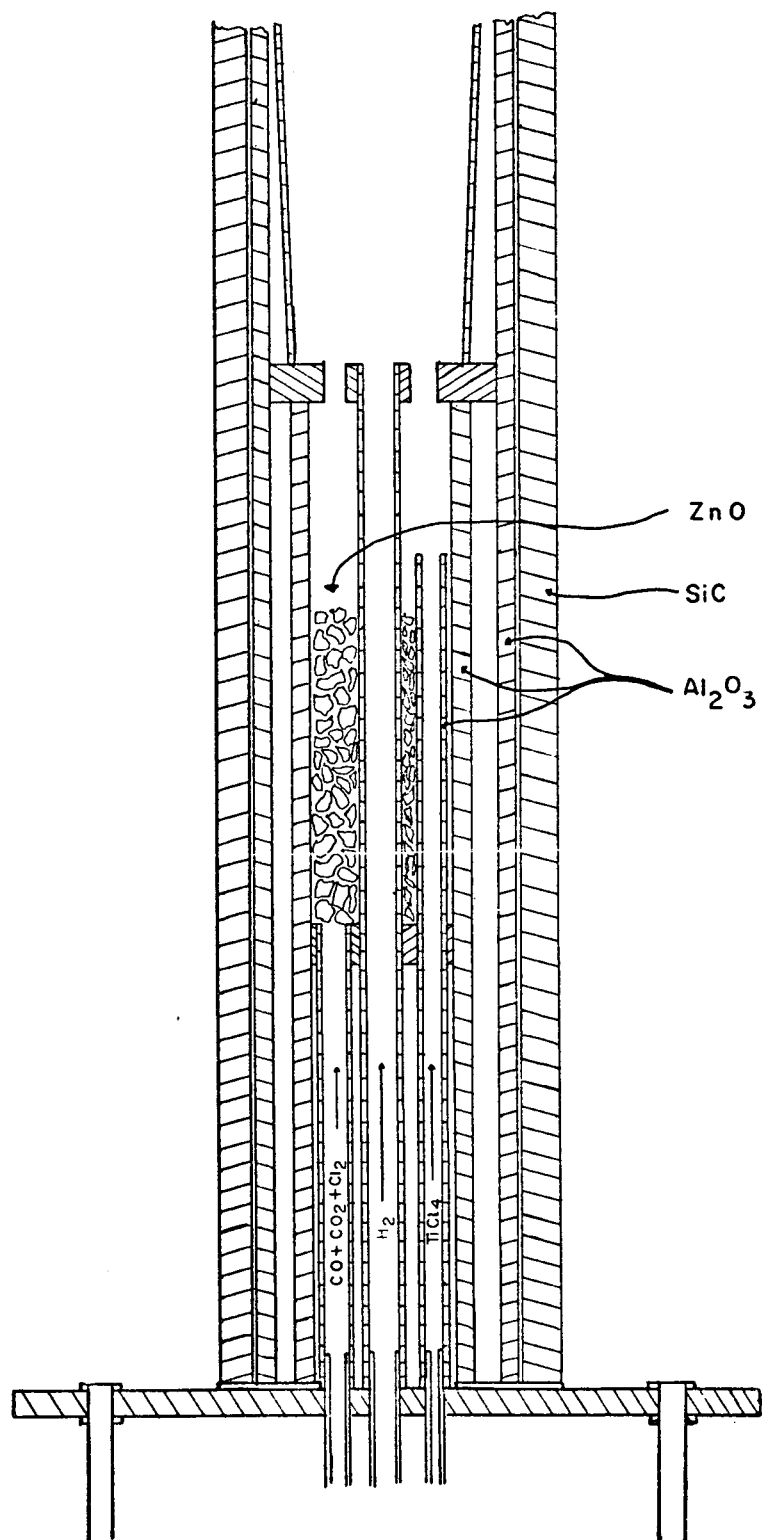Figure 15.   Reactor Mixing Performance for Zn_2TiO_4 Production

29

Figure 16. Modified SiC Furnace Reactor

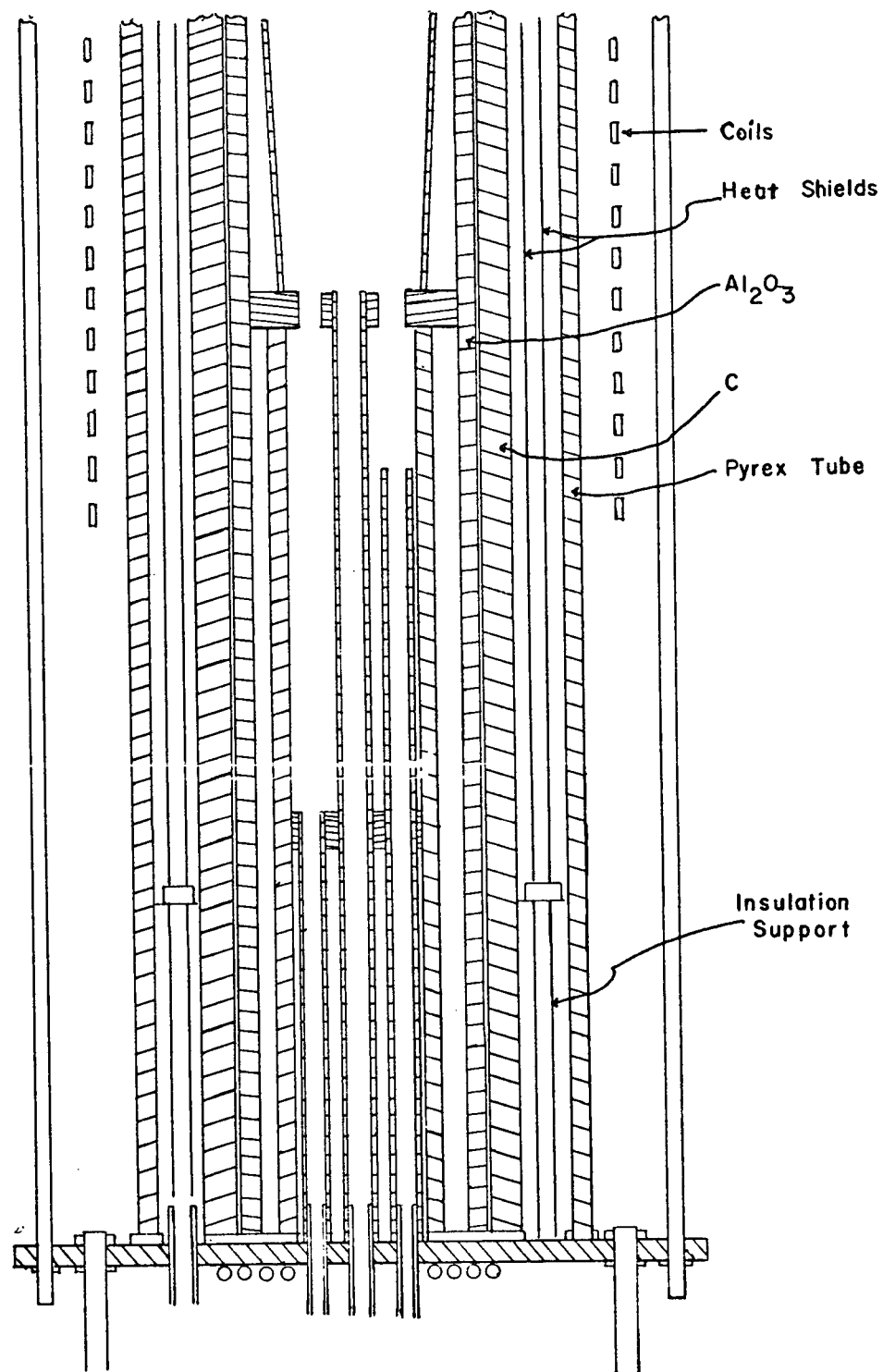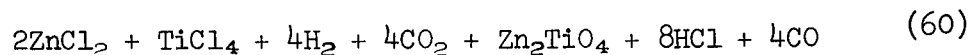Figure 17.   Induction Furnace Reactor

III. EXPERIMENTAL RESULTS

Zinc Orthotitanate

Formation of Zn_2TiO_4 from homogeneous nucleation in the vapor phase was attempted using the following reaction:

$$2ZnCl_2 + TiCl_4 + 4H_2 + 4CO_2 + Zn_2TiO_4 + 8HCl + 4CO \qquad (60)$$

The silicon carbide tube furnace was used with hydrogen injected through the central injector tube. Titanium chloride was injected through the alumina tube above the ZnO chlorinator and Cl_2, CO and CO_2 were injected into the ZnO chlorinator. System conditions and phase analysis for the Zn_2TiO_4 runs are summarized in Table 3.

Powder was deposited on the wall of the reaction tube above the hot zone (Zone #1) and on the metal Tee above the reaction tube (Zone #2). Traces of Zn_2TiO_4 were deposited in Zone #1 along with ZnO in run 1 and ZnO and $ZnCl_2$ in run 2.

TABLE 3: Zn_2TiO_4 RUN CONDITIONS

	Run	1	2
Temperature °C		1495	1450
Cl_2 to ZnO	(cc/min)	45	100
Cl_2 to Ti	(cc/min	45	50
CO	(cc/min)	100	100
CO_2	(cc/min)	100	50
H_2	(cc/min)	200	200
Total Pressure	(mmHg)	150	350
Phase Analysis	Zone 1	(1) ZnO (2) Zn_2TiO_4 (Tr)	(1) ZnO (2) $ZnCl_2$ (3) Zn_2TiO_4 (Tr)
	Zone 2	(1) $ZnCl_2$	(1) $ZnCl_2$ (2) Zn

CONCLUSIONS

1. Mixing calculations and reactor design should provide conditions for adequate mixing of the reactant gases.

2. Zinc orthotitanate powder was produced using the modified reactor.

REFERENCES

1. Campbell, W. B., et al, "Preparation of Pigments for Space-Stable Thermal Control Coatings". The Ohio State University Research Foundation, NASA Contract No. NAS 8-21317, July 1969.

2. Campbell, W. B., et al., "Preparation of Pigments for Space-Stable Thermal Control Coatings". The Ohio State University Research Foundation, NASA Contract No. NAS 8-21317, July 1970.

3. Bird, R. B., Stewart, W. E., Lightfoot, E. N. Transport Phenomena, p. 23, J. Wiley (1960).

4. Bird, R. B., Loc. Cit., p. 746.

5. Wilke, C. R., J. Chem. Phys., 18, pp. 517-519 (1950)

6. Bird, R. B., Loc. Cit., p. 259.

7. Bird, R. B., Loc. Cit., p. 511.

8. Campbell, W. B., et al., Loc. Cit., p. 45, July 1970.

9. Schlichting, H., Boundary Layer Theory, p. 168, McGraw-Hill (1960).

10. Brodkey, R. S., The Phenomena of Fluid Motions, p. 327, Addison-Wesley (1967).

11. Lee J. and Brodkey, R. S., "Turbulent Motion and Mixing in a Pipe", A.I.Ch.E. Journal 10, pp. 187-193 (1964).

12. Gegner, J. P., and Brodkey, R. S., "Dye Injection at the Centerline of a Pipe", A.I.Ch.E. Journal 12, pp. 817-819 (1966).

13. Brodkey, R. S., "Turbulent Motion, Mixing and Kinetics". Professional Development Lectures. Vol. 1, No. 2, November 1968, West Virginia University, Nitro, W. Va.

14. Pai, S. I., "On Turbulent Jet Mixing of Two Gases at Constant Temperature". J. of Appl. Mech., pp. 41-47, March (1955).

15. Corrsin, S., A.I.Ch.E. Journal 3, p. 329 (1957)

16. Ibid. 10, p. 870 (1964).

17. Danchwerts, I. V., Chem. Eng. Sci. 8, p. 93 (1958).

18. Bordkey, R. S., The Phenomena of Fluid Motions, Loc. Cit., p. 331.

19. Brodkey, R. S., "Turbulent Motion, Mixing and Kinetics", Op. Cit.

20. Brodkey, R. S., "Turbulent Motion, Mixing and Kinetics", Op. Cit.

21. Wilke, C. R., Op. Cit.

22. Hinze, J. O., "Non-isotropic Free Turbulence", Chapter 6, Turbulence, McGraw-Hill (1959).

23. Champagne, F. H. and Wygnanskii, I. J., "Coaxial Turbulent Jets". Boeing Sci. Res. Lab. Document D1-82-0958. Flight Sciences Laboratory, February 1970.

24. Hinz, J. O., Op. Cit.

25. Ibid

26. Champagne, F. H., Op. Cit

27. Ibid

28. Hinz, Loc. Cit., p. 425

29. Bordkey, R. S., O.S.U. Chemical Engineering Department, Private Communication.